International Journal of Mass Spectrometry 301 (2011) 55–61

Contents lists available at ScienceDirect

International Journal of Mass Spectrometry

journal homepage: www.elsevier.com/locate/ijms

Proper and improper aminoketyl radicals in electron-based peptide dissociations

Thomas W. Chung, František Tureček*

Department of Chemistry, University of Washington, Bagley Hall, Box 351700, Seattle, WA 98195-1700, United States

ARTICLE INFO

Article history:
Received 28 March 2010
Received in revised form 21 June 2010
Accepted 22 June 2010
Available online 30 June 2010

Keywords:
Electron transfer dissociation
Radical migration
z-Type ions
Ab initio calculations
Collision-induced dissociation

ABSTRACT

Two types of aminoketyl radicals and cation-radicals are distinguished by each's structure and reactivity. As proper aminoketyl radicals we denote the presumed intermediates of N—C_α bond dissociations induced by electron attachment to protonated peptides. These radicals have pyramidized aminoketyl groups, —$C_\alpha C^\bullet(OH)NH$—, high spin density on the central carbon atom, and undergo facile N—C_α bond dissociations. The critical energies for N—C_α bond cleavages in proper aminoketyl radicals are summarized here and typically do not exceed 60 kJ mol^{-1} in peptide cation-radicals. In contrast, a different type of intermediates, which we call improper aminoketyl radicals, is formed by collisional dissociation of peptide cation-radicals, such as decarboxylation of $\mathbf{z}_n$ fragments. Improper aminoketyl radicals have near planar —$C_\alpha C(OH)NH$— groups, and the spin density is delocalized over several atoms adjacent to the aminoketyl moiety. Improper aminoketyl radicals show higher transition energies for N—C_α bond cleavage and undergo H-atom transfers resulting in side-chain losses.

1. Introduction

Aminoketyl radicals, R—$C^\bullet$(OH)—NH—R, are transient organic species that arise by hydrogen atom addition to amides, hydroxyl radical addition to imines, or related radical additions. Aminoketyl radicals are thought to play a role of reactive intermediates in DNA and RNA damages due to redox and radical reactions involving cytosine and uracil nucleobases, respectively [1]. Peptide-related aminoketyl radicals have been invoked as reactive intermediates in backbone dissociations induced by electron attachment to gas-phase ions produced by single or multiple protonation by electrospray ionization [2]. Three amide-related aminoketyl radicals, $HC^\bullet(OH)NH_2$ [3], $CH_3C^\bullet(OH)NH_2$ [4], and $CH_3C^\bullet(OH)NHCH_3$ [5], have been unequivocally generated in the gas phase from the corresponding cations of well-defined structures that were reduced by femtosecond collisional electron transfer [6]. The interest in aminoketyl radical stems from their reactivity, for the radical center substantially weakens the adjacent O—H and N—C bonds to undergo homolytic dissociation. For example, the O—H and N—CH_3 bond dissociation energies (BDE) in $CH_3C^\bullet(OH)NHCH_3$ have been calculated at high levels of theory to be 31 and 11 kJ mol^{-1}, respectively [5], and involved energy barriers of 84–86 kJ mol^{-1} in the respective transition states (TS). These are substantially lower than the typical homolytic BDE of O—H (430 kJ mol^{-1}) and N—CH_3 bonds (335 kJ mol^{-1}) in alcohols and amines [7]. Both the BDE and TS energies further decrease when the departing C-based radical is stabilized by odd-electron delocalization in a conjugate π-system. This feature is of a particular importance in dissociations of peptide radicals and cation-radicals where N—C_α bond dissociations produce specific amide C_α radical fragments that are the basis of sequence analysis.

Scheme 1 illustrates N—C_α bond dissociations in a cation-radical produced by electron transfer to a doubly protonated model pentapeptide AAHAL which forms N-terminal fragment ions (denoted $\mathbf{c}^+$ ions) [2] and C-terminal fragment ions ($\mathbf{z}^{+\bullet}$ ions). Although experimental energy measurements are not yet available for dissociations of charge-reduced peptides, TS and BDE have been calculated for several N—C_α bond dissociations in peptide radicals, cation-radicals, and related model amide systems (Table 1). We call such aminoketyl radicals *proper*, because they share important electronic and structural properties. One is the prevalent (>95%) concentration of *odd-electron density* within the $C^\bullet$(OH)NH moiety, with a major localization at the amide carbon atom [8]. The other distinct property is the substantial *pyramidization* of the pertinent carbon atom which, when expressed as the out-of-plane deflection of the OH group from the plane defined by the C_α, $C^\bullet$, and N atoms (C_α—C—N plane), is typically 40–45° for proper aminoketyl radicals [9].

Peptide radicals and cation-radicals have been of much recent interest regarding the formation of various transient radical species in crystals [10] and the gas phase [11,12]. Peptide radicals and cation-radicals have been reported to undergo rearrangements by hydrogen atom migrations. Thus, electron attachment to arginine [13] and histidine containing peptide ions [14] has been found to trigger hydrogen atom migrations onto these side-chain moieties. Hydrogen atom migrations have been observed to occur between

* Corresponding author. Tel.: +1 206 685 2041; fax: +1 206 685 3478.
E-mail address: turecek@chem.washington.edu (F. Tureček).

1387-3806/$ – see front matter © 2010 Elsevier B.V. All rights reserved.
doi:10.1016/j.ijms.2010.06.025

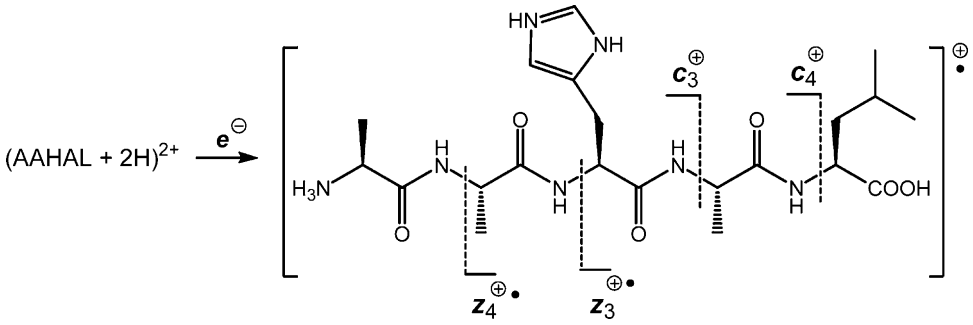

Scheme 1.

incipient **c** and **z** backbone fragments [15] and involved alkyl side-chain groups [16]. Hydrogen-deficient peptides generated by redox reactions [17,18] and hydrogen atom abstraction reactions [19] have also been reported to undergo hydrogen atom migrations.

In this context, recent studies of peptide cation-radicals, generated by methods other than direct electron attachment, revealed another type of stable aminoketyl radicals that did not induce N—C_α bond dissociations when they were subjected to collisional activation [20]. The goal of this work is to analyze the properties and reactivity of selected representatives of what we call *improper* aminoketyl radicals. The differences between the proper and improper aminoketyl radicals will be highlighted by analyzing their electronic properties and comparing their dissociation energetics and kinetics.

2. Experimental

2.1. Methods

Peptides AHDAL and AHADL (95% pure) were purchased from GenScript (Piscataway, NJ) and used as received. AHAAL (98% pure) was purchased from NEO-Group (Cambridge, MA). Electron transfer dissociation mass spectra were obtained on a Thermo Fisher LTQ XL linear ion trap mass spectrometer equipped with an electrospray ion source and a chemical ionization source for the production of fluoranthene anion radicals. Peptide ions were produced by electrospray from 5 to 10 μM solutions in 50/50 methanol–water containing 1% of acetic acid. Doubly charged ions, $(AHDAL+2H)^{2+}$, *m/z* 263.5, $(AHADL+2H)^{2+}$, *m/z* 263.5, and $(AHAAL+2H)^{2+}$, *m/z* 241.5, were accumulated in the ion trap and selected by their mass to charge ratios. The mass selection window was 2 *m/z* units to include nearest ^{13}C isotopologues. Electron transfer dissociation was accomplished at 100 and 200 ms ion–ion interaction time. $\mathbf{z_4}$-Ions from ETD (*m/z* 439) were mass-selected and collisionally dissociated (MS^3). The ion excitation energy was set at 20–35% on the instrument scale. The decarboxylated $\mathbf{z_4}$ ions at *m/z* 395 were mass selected and subjected to collisional activation to yield the MS^4 spectrum reported here.

2.2. Calculations

Standard ab initio and density functional theory calculations were performed using the Gaussian 03 suite of programs [21]. Geometries were optimized with the hybrid B3LYP functional [22] using the 6-31+G(d,p) basis set. Initial guesses for the cation-radical structures were taken from a previous study [20]. Exhaustive conformational searches are currently not feasible for cation-radicals because of the lack of a suitable force field. Stationary points were characterized by harmonic frequency calculations to identify local energy minima (all real frequencies) and first-order saddle points (one imaginary frequency). Additional sets of energies were obtained by single-point calculations using B3LYP and the Møller–Plesset perturbational theory [23] (second order, frozen core) with the larger 6-311++G(2d,p) basis set. Calculations on all open-shell species (radicals and cation-radicals) used the spin-unrestricted formalism. Spin contamination was quite modest in most cases and was treated by Schlegel's spin annihilation protocol [24]. The B3LYP and spin-projected MP2 (PMP2) energies were averaged (B3–PMP2) to compensate for small errors inherent to both approximations according to the procedure reported previously [25]. Spin and charge densities were calculated using Natural Population Analysis [26]. Unimolecular rate constants were calculated using the Rice–Ramsperger–Kassel–Marcus (RRKM) theory [27] and employing a modified Hase's program [28] which was recompiled for Windows XP [29]. The RRKM rate constants were obtained by direct count of quantum states at internal energies that were increased in 2 kJ mol^{-1} steps from the transition state up to 400 kJ mol^{-1} above the reactant. Rotations were treated adiabatically and the calculated microscopic rate constants $k(E,J,K)$ were

Table 1
Calculated bond dissociation (BDE) and transition state (TS) energies for N—C_α bond dissociations in proper aminoketyl radicals.

Species	Energy[a]		
	BDE	TS	Ref.
$CH_3C^\bullet(OH)NH—CH_3$	11	84	[5]
$H_2NCH_2CH_2C^\bullet(OH)NH—CH_3$	23	95	[9b]
$CH_3C^\bullet(OH)NH—CH_2CH_2NH_2$	38	76	[8]
$CH_3C^\bullet(OH)NH—CH_2CH_2NH_3^+$	76[b]	66	[8]
$CH_3C^\bullet(OH)NH—C_\alpha H$-Lys	−12	42	[8]
$H_2NCH_2C^\bullet(OH)NH—CH_2CONH_2$	−1(9)[c]	37–71[c]	[8]
$H_3N^+CH_2C^\bullet(OH)NH—CH_2CONH_2$	67[b]	40	[8]
$H_2NCH_2C^\bullet(OH)NH—C_\alpha H$-ArgH$^+$	7–24[b,c]	5–52[b,c]	[13]
Pro-C$^\bullet$(OH)NH—CH_2COOH	18	52	[35]
Gly-Pro-C$^\bullet(OH)_2$	−89[d]	50[d]	[35]
$H_2NCH_2C^\bullet(OH)NH—C_\alpha$HPro	−15[d]	39[d]	[35]
$H_2NCH_2C^\bullet(OH)NH—C_\alpha$HLysH$^+$	−39[b]	7–47[b,c]	[36]
H^+LysCONH—$C_\alpha HC^\bullet(OH)_2$Lys	−9[b]	40[b]	[36]
H^+GlyNH—$C_\alpha{}^\bullet H(OH)NH_2(CH_2Ph)$	−25[b]	2[b]	[30]
AlaC$^\bullet$(OH)NH—C_αHAla-HisH$^+$-Ala-Leu	–[e]	59	[32]
Ala-AlaC$^\bullet$(OH)NH—C_αHHisH$^+$-Ala-Leu	–[e]	42	[32]
Ala-Ala-HisH$^+$C$^\bullet$(OH)NH—C_αHAla-Leu	–[e]	33	[32]
Ala-Ala-HisH$^+$-AlaC$^\bullet$(OH)NH—C_αHLeu	–[e]	23	[32]
4 → **TS3**	89[b]	95	[g]
4 → **TS4**	43[f]	73	[g]
5 → **TS5**	164[b]	86	[g]

[a] In units of kJ mol^{-1} from combined single-point B3LYP and PMP2/6-311++G(2d,p) energies and including B3LYP/6-31+G(d,p) zero-point vibrational energies.
[b] These dissociations involve stable ion–molecule complexes as intermediates.
[c] Energy ranges for different conformers.
[d] N—C_α bond cleavage in the proline ring.
[e] BDE vary depending on the formation of amide or enolimine **c** fragments.
[f] Reaction enthalpy for **4** → **4c**.
[g] This work.

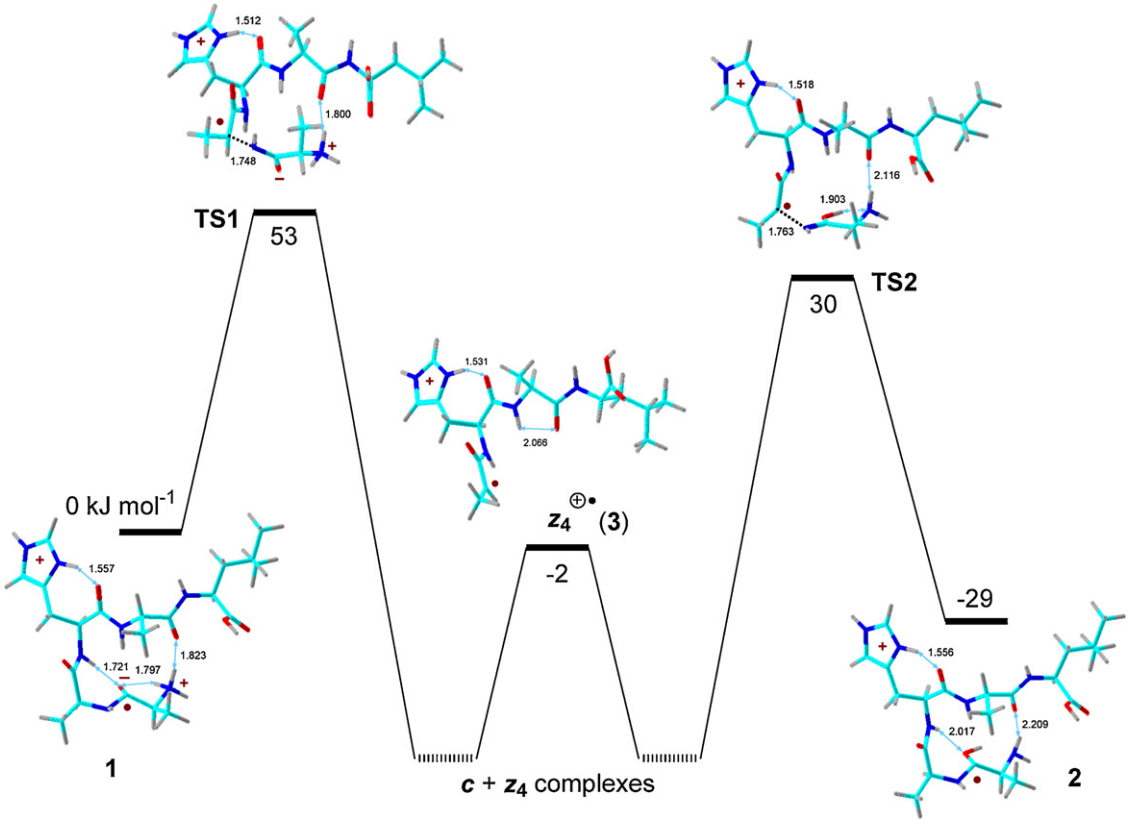

Fig. 1. Potential energy diagram for N—C_α bond dissociations in $(AAHAL+2H)^{+\bullet}$ cation-radical. The relative energies are from combined B3LYP and PMP2/6-311++G(2d,p) single point energy calculations and include B3LYP/6-31+G(d,p) zero-point corrections.

then Boltzmann-averaged over the thermal distribution of rotational states at 298 K.

3. Results and discussion

3.1. Aminoketyl radicals by electron transfer

Fig. 1 shows a calculated potential energy diagram for an N—C_α bond dissociation in a proper aminoketyl cation-radical from electron transfer dissociation of $(AAHAL+2H)^{2+}$. Electron attachment to the doubly charged ion forms a zwitterionic state of the cation-radical (**1**) which can undergo an exothermic proton transfer isomerization to aminoketyl cation-radical **2**. This proton transfer requires a very low TS energy (not shown in Fig. 1). Competing with proton transfer in **1** is the N—C_α bond dissociation through **TS1** which is accompanied by proton transfer yielding the $\mathbf{z_4}$ fragment ion (**3**) and alanine amide or enolimine as the neutral $\mathbf{c_1}$ fragment. The aminoketyl cation-radical **2** can form ion **3** by N—C_α bond dissociation through **TS2**. It should be noted that the reaction paths from **TS1** and **TS2** involve ion–molecule complexes between ion **3** and the neutral alanine fragment. A few (**c** + **z**) ion-molecule complexes have been characterized so far [30]; their general feature is that as a rule they are more stable than both the aminoketyl reactants and the separated **c** and **z** fragments, and they can facilitate isomerization of **c**-fragment enolimine groups to the much more stable amide groups [31]. Fig. 1 illustrates structure **2** as a proper aminoketyl cation-radical. It is pyramidized at the Ala_1 aminoketyl carbon atom with the OH group at 42° out of the C_α–C–N plane. The aminoketyl group carries 92% of spin density out of which 75% is at the carbon atom.

3.2. Aminoketyl radicals by ion dissociations

We now consider the reactions of two isomeric aminoketyl radicals (**4** and **5**, Scheme 2) which are structurally different from **2**. Ion **4** was formed in three steps from $(AHDAL+2H)^{2+}$. The first step was electron transfer that induced a dissociation of the N—C_α bond between the Ala and His residues forming a $\mathbf{z_4}$ ion ($^\bullet$HDAL$^+$, Scheme 2) [32]. This ion was isolated and collisionally activated to eliminate CO_2 from the Asp residue forming ion **4**. Ion **4** is denoted as $^\bullet$H$\underline{A}$AL$^+$, where $\underline{A}$ stands for the decarboxylated Asp residue which is isomeric with an Ala residue. It should be noted that of several reaction paths for the CO_2 elimination from $^\bullet$HDAL$^+$, the one involving the Asp COOH group and leading to **4** was found to be energetically and kinetically preferred [20]. Ion **5** represents a higher energy tautomer of **4** ($\Delta H_{g,0}(\mathbf{4}\rightarrow\mathbf{5}) = 46$ kJ mol^{-1}) which has an aminoketyl moiety at the former His amide group, and is used here only for comparison of their properties.

Collision-induced dissociation of **4** results in the formation of two kinds of fragments (Fig. 2a). One series is due to losses of small molecules and radicals, e.g., water (*m/z* 377), $C_3H_7^\bullet$ (*m/z* 352), CO_2 (*m/z* 351), C_4H_8 (*m/z* 339), and their combinations (*m/z* 333, 308, 295, etc.). The other series consists of N-terminal truncated **b** ions, denoted here as $^t\mathbf{b_3}$ (*m/z* 264) and $^t\mathbf{b_2}$ (*m/z* 193), that are formed by amide bond cleavages, and backbone fragments at *m/z* 220, 210, and 203 (Fig. 2). Also of note is that the $^t\mathbf{b_3}$ and $^t\mathbf{b_2}$ ions are accompanied by $^t\mathbf{b_3}$ +1 and $^t\mathbf{b_2}$ +1 satellites indicating hydrogen atom transfers to the charged fragments. The formation of the *m/z* 220 and 210 ions is less clear, although it should be noted that these fragment ions also appear in the CID spectra of $\mathbf{z_5}$ and $\mathbf{z_4}$ ions from ETD–CID–MS^3 of AHDAL, AHADL, AAHAL, and AHAAL peptide ions [20], and pre-

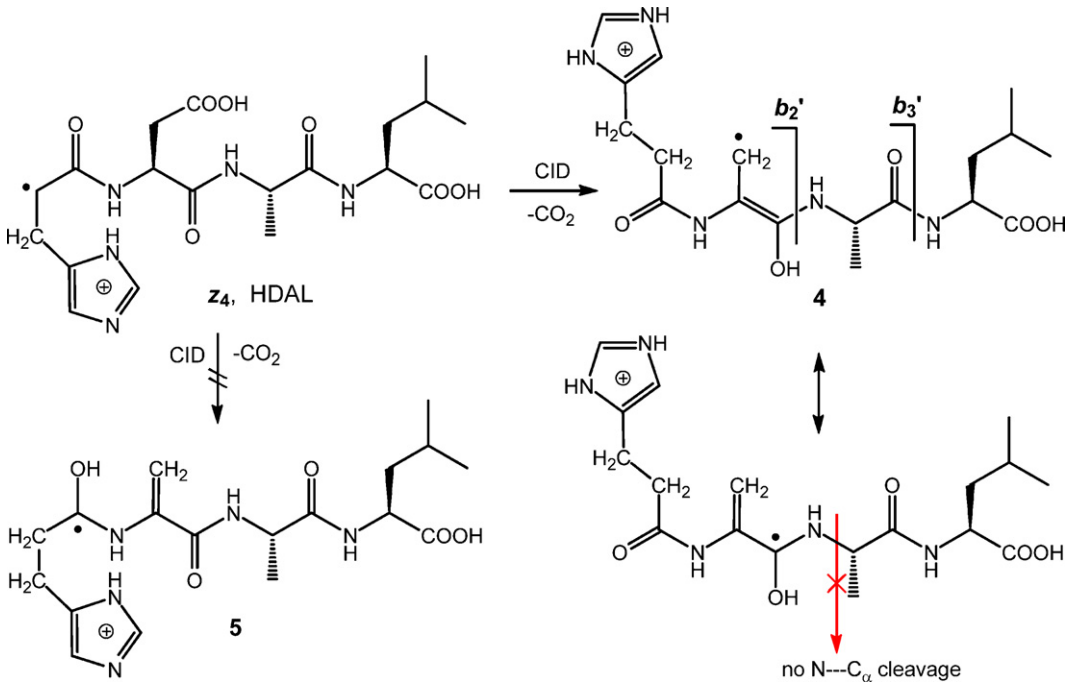

Scheme 2.

sumably consist of truncated sequences after decarboxylation or side-chain losses.

Two *m/z* 395 ions isomeric with **4** were generated by separate fragmentation sequences. Ion **6a**, denoted as •HA<u>A</u>L, was produced from $(AHADL+2H)^{2+}$ by an ETD–MS^3 sequence analogous to that for the formation of **4**, e.g., $(AHADL+2H)^{2+} \rightarrow$ •HADL (*m/z* 439) → HA<u>A</u>L. Ion **6b** was produced as a regular $\mathbf{z_4}$ fragment by ETD of $(AHAAL+2H)^{2+}$ and is denoted here as •HAAL. The CID spectra of ions **6a** and **6b** (Fig. 2b and c, respectively) show very similar fragment ions as does the CID spectrum of **4**. The CID spectra are dominated by ions due to radical-induced loss of C_3H_7 and further display fragments due to eliminations of water, CO_2, C_4H_8, combinations thereof, and common $^t\mathbf{b_2}$ and $^t\mathbf{b_2}$ sequence ions at *m/z* 193 and 264, respectively. This overall similarity indicates that upon collisional activation the formerly isomeric ions **4**, **6a**, and **6b** interconverted by hydrogen atom migrations to a mixture of common radical intermediates.

However, the CID spectra in Fig. 2 show neither a His-truncated $^t\mathbf{c_2}$ fragment ion at *m/z* 209 from •H<u>A</u>AL nor a $^t\mathbf{c_3}$ fragment ion at *m/z* 280 from •HA<u>A</u>L that would be the expected products of N—C_α bond dissociations at the <u>A</u> residue in aminoketyl radicals **4** and **6a**, respectively. Hence, the lack of these fragments indicates that N—C_α bond cleavage was competitive neither with the radical-induced side-chain dissociations, nor with the charge-induced backbone fragmentations of **4** and **6**. The question is: why?

We address this question by analyzing the energetics of N—C_α bond cleavage in **4**. Scheme 3 shows the optimized structure of **4** and select transition states for its dissociations and isomerizations. Cation-radical **4** has a near planar enolimine system where the OH group is only 0.8° out of the C_α–C–N plane. Note that structure **4** has a cis amide bond which is favorable for facilitating hydrogen atom transfers along the peptide backbone [20]. The odd-electron density is delocalized among the Asp C_β carbon which carries 60% and atoms of the aminoketyl group (40%). However, the spin density on the central enolimine carbon in **4** is only 36% as opposed to proper aminoketyl radicals where the central carbon atoms typically carry ≥75% of spin density [9].

The N—C_α bond dissociation in **4** requires 95 kJ mol^{-1} in **TS3** (Scheme 3). Although this TS energy is higher than those for proper aminoketyl radicals (Table 1), it is still lower than the typical TS energies for proton-induced backbone dissociations in peptide ions (120–150 kJ mol^{-1}) [33]. The N—C_α bond dissociation through **TS3** leads to an ion-radical complex **4a** which is 32 kJ mol^{-1} above **4**.

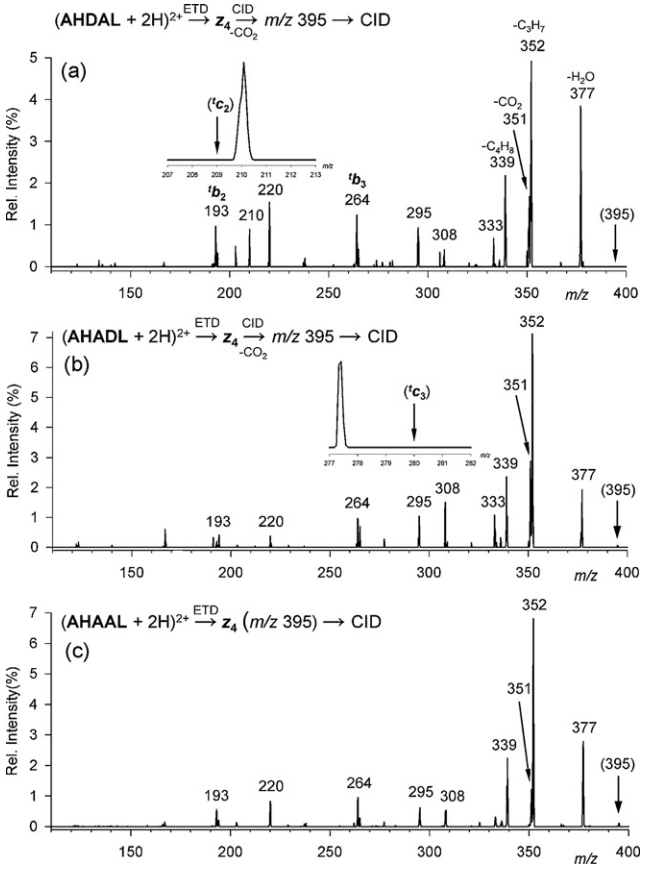

Fig. 2. ETD–CID–MS^4 mass spectra of the *m/z* 395 ions from (a) **4**, (b) **6a**, and (c) **6b**. Insets show expanded *m/z* regions with putative $^t\mathbf{c_2}$ and $^t\mathbf{c_3}$ sequence fragment ions.

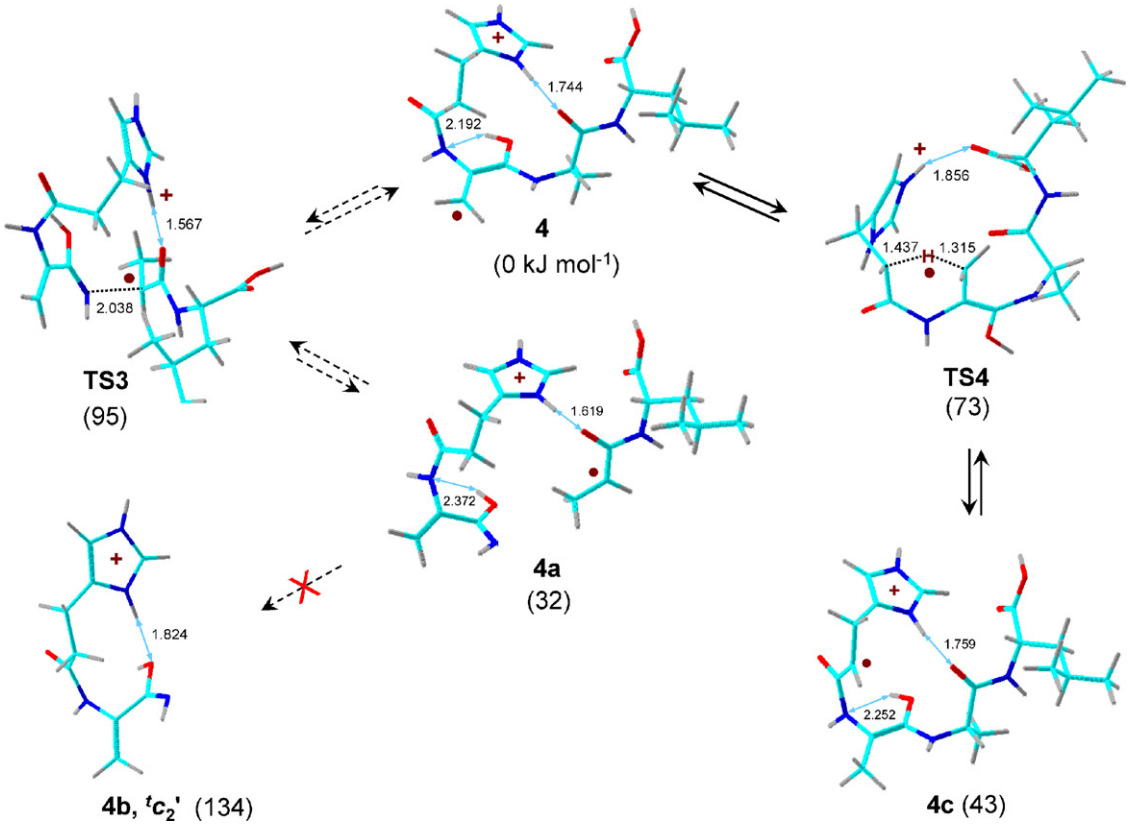

Scheme 3.

Further dissociation of **4a** to the putative $^{t}\mathbf{c_2}$ ion and $\mathbf{z_2}$ radical is substantially endothermic and the dissociation energy depends on the $^{t}\mathbf{c_2}$ ion structure. The formation of a $^{t}\mathbf{c_2}$ ion with an anti-anti-enolimine group (**4b**), which correlates with **TS3**, requires 134 kJ mol^{-1}. Although the incipient product **4b** can isomerize to more stable enolimine or amide isomers in complex **4a** [20], the dissociation pathway is made unfavorable by the high energy in **TS3**.

Instead of dissociating, cation-radical **4** can undergo competitive H-atom transfers to the former Asp C_β methylene which shows a pronounced radical character. One such rearrangement involves H-transfer from the His C_α position through **TS4** which requires 73 kJ mol^{-1} and converts ion **4** to a •HAAL $\mathbf{z_4}$ isomer (**4c**). The **4** → **4c** isomerization is 43 kJ mol^{-1} endothermic and thus reversible. The higher stability of **4** compared to **4c** can be attributed to its planar CH_2—C=C(OH)—N π-conjugated system which is replaced by a shorter CH—CO—NH π-conjugated system of **4c**. Note that interaction of the His and modified Asp (A) π-systems in both **4** and **4c** is hampered by unfavorable dihedral angles about the His-NH—Asp′-C_α bonds which are 84° and 70°, respectively.

In addition to the **4** ↔ **4c** isomerization, both cation-radicals can undergo further H-atom migrations involving C_α-H atoms of the Ala and Leu residues, the COOH group and the Leu side chain. Although we did not study all these rearrangements for **4** and **4c**, a previous investigation of H-atom migrations in $\mathbf{z_4}$ ions indicated that such H-atom migrations are facile and lead to intermediates for eliminations of CO_2, C_3H_7, and C_4H_8 [20] which are the major dissociations of **4** (Fig. 2).

The difference in the **TS3** and **TS4** energies is reflected in the rate constants calculated by RRKM on the combined B3LYP and PMP2/6-311++G(2d,p) potential energy surface (Fig. 3). The rate constant for H-atom migration (k_{mig}) is consistently larger than that for the N—C_α bond cleavage ($k_{N–C}$). Both rate constants show a substantial kinetic shift to reach the value needed

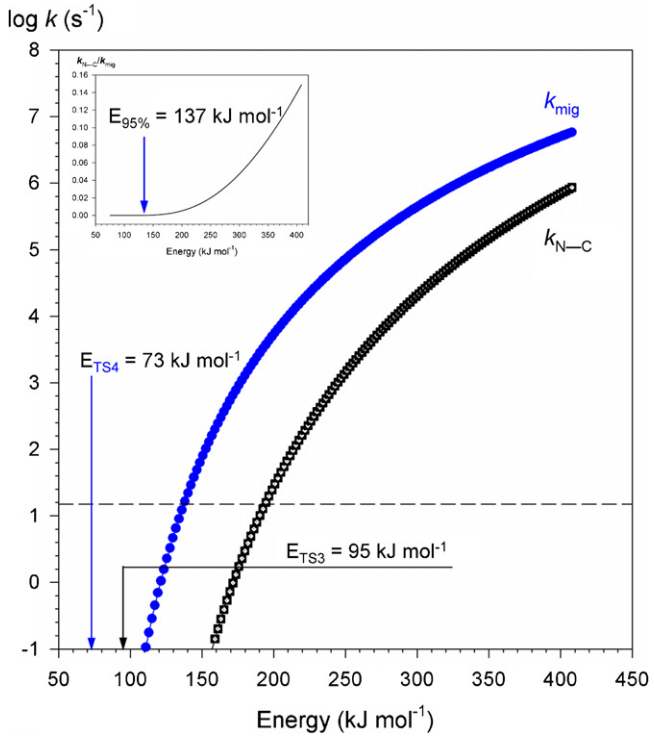

Fig. 3. RRKM rate constants (log k, s^{-1}) of dissociations of **4** by N—C_α bond dissociation (**TS3**, $k_{N–C}$, black open squares) and H-atom migration (**TS4**, k_{mig}, blue full circles). The dashed line is drawn at k allowing 95% dissociation on the 200 ms experimental time scale. Inset shows the branching ratio for $k_{N–C}/k_{mig}$ as a function of internal energy. The arrow in the inset indicates the internal energy needed for 95% H-atom migration on the 200 ms time scale. (For interpretation of the references to color in this figure legend, the reader is referred to the web version of this article.)

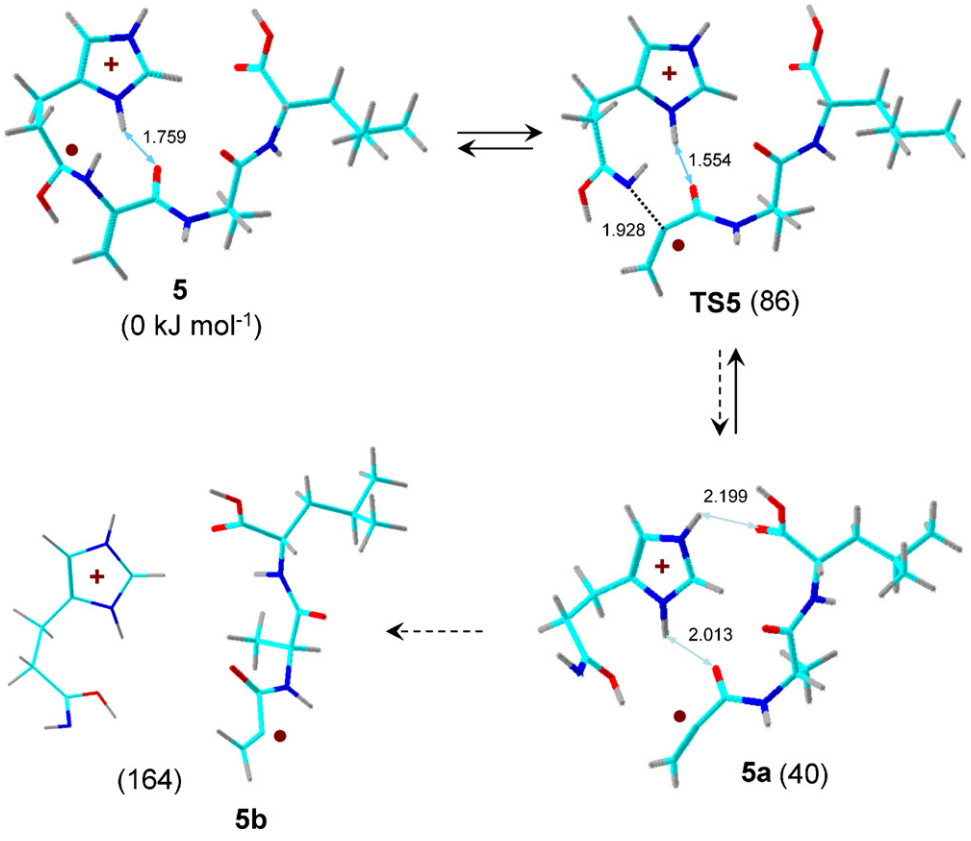

Scheme 4.

for 95% dissociation on the experimental time scale of 200 ms ($k = 15\ s^{-1}$, log $k = 1.17$), as indicated by a broken line in Fig. 3. For k_{mig} this occurs at 137 kJ mol^{-1} reactant internal energy indicating a 137–73 = 64 kJ mol^{-1} kinetic shift. For $k_{N–C}$ this occurs at 194 kJ mol^{-1} indicating a 194–95 = 99 kJ mol^{-1} kinetic shift. The inset in Fig. 3 shows the branching ratio for the two dissociations, $k_{N–C}/k_{mig}$. At an internal energy where k_{mig} can account for 95% reaction (137 kJ mol^{-1}), the RRKM calculated $k_{N–C}/k_{mig}$ branching ratio is 1×10^{-4}. This is consistent with the CID spectrum of **4** which shows no N—C_α bond cleavage to compete with dissociations triggered by H-atom migrations.

The optimized structure of cation-radical **5** shows a pyramidized aminoketyl group where the OH group is 48° out of the C_α—C—N plane (Scheme 4). The spin density is mostly (94%) confined in the aminoketyl group. Thus, according to its geometrical and electronic structure, cation-radical **5** is a proper aminoketyl radical. Despite this feature, an N—C_α bond dissociation of **5** requires a relatively high-energy transition state in **TS5** (86 kJ mol^{-1}, Table 1) and forms an ion-molecule complex (**5a**) which is 40 kJ mol^{-1} less stable than reactant **5** (Scheme 4). In this case, the resistance to N—C_α bond dissociation can be ascribed to the formation of a vinyl radical system, CH_2=C•—C(=O)—NH, in the neutral fragment **5b**. Since this is a σ-radical, it lacks conjugation of the CH_2=C• and C(=O)—NH groups and hence the high energy for the product formation (164 kJ mol^{-1}), as well as for the pertinent transition state (**TS5**).

It may be noted that the presence of some π−conjugated groups in peptide ions has been reported to hamper N—C_α bond dissociations upon electron capture or transfer [13,14,34]. The interfering groups had high H-atom affinities and were considered H-atom traps. The present data indicate that the conjugated acrylic CH_2=C—C(OH)—N system can also be considered an H-atom trap. The data also indicate that competition between H-atom trapping and N—C_α bond dissociation is a kinetic not thermodynamic effect. While the **4** → **4a** dissociation is less endothermic than the **4** → **4c** H-atom migration, the latter is preferred by its lower TS energy. This feature indicates that studies of H-atom migrations in peptide cation-radicals must address TS energies by theory and experiment to provide a realistic picture of competing fragmentations.

4. Conclusions

Two types of aminoketyl radicals are distinguished by their structure, electronic properties, and reactivity. Proper aminoketyl radicals have pyramidized C_α—C(OH)—N geometries and carry most of the spin density in the pivot carbon atom of the aminoketyl group. Proper aminoketyl radicals correspond to transient intermediates of dissociations of charge-reduced peptide ions in ECD and ETD and exhibit low transition state energies for N—C_α bond dissociations. We identify improper aminoketyl radicals as species that have C_α—C(OH)—N groups that are conjugated to adjacent π-electronic systems. This results in delocalization of spin density away from the pivot aminoketyl carbon atom, changes the aminoketyl group geometry, and substantially elevates TS energies for N—C_α bond dissociations.

Acknowledgements

The authors thank Dr. Priska von Haller of the University of Washington Proteomics Resource Center for access to the Thermo LTQ XL instrument. Research support by the NSF (Grants CHE-0750048 for experiments and CHE-0342956 for computations) is gratefully acknowledged. The Department of Chemistry Computer Facility has been jointly supported by the NSF and University of Washington.

References

[1] C. von Sonntag, Adv. Quant. Chem. 52 (2007) 5.
[2] R.A. Zubarev, N.L. Kelleher, F.W. McLafferty, J. Am. Chem. Soc. 120 (1998) 3265.
[3] E.A. Syrstad, F. Tureček, J. Phys. Chem. A 105 (2001) 11144.
[4] F. Tam, E.A. Syrstad, X. Chen, F. Tureček, Eur. J. Mass Spectrom. 10 (2004) 869.
[5] E.A. Syrstad, D.D. Stephens, F. Tureček, J. Phys. Chem. A 107 (2003) 115.
[6] F. Tureček, Top. Curr. Chem. 225 (2003) 77.
[7] D.F. McMillen, D.M. Golden, Ann. Rev. Phys. Chem. 33 (1982) 493.
[8] F. Tureček, J. Am. Chem. Soc. 125 (2003) 5954.
[9] (a) F. Tureček, E.A. Syrstad, J. Am. Chem. Soc. 125 (2003) 3353;
(b) C. Yao, E.A. Syrstad, F. Tureček, J. Phys. Chem. A 111 (2007) 4167.
[10] Y. Zhou, W.H. Nelson, J. Phys. Chem. B 114 (2010) 5567.
[11] T. Ly, R.R. Julian, J. Am. Chem. Soc. 130 (2008) 351.
[12] V. Ryzhov, A.K.Y. Lam, R.A.J. O'Hair, J. Am. Soc. Mass Spectrom. 20 (2009) 985.
[13] S. Panja, S.B. Nielsen, P. Hvelplund, F. Tureček, J. Am. Soc. Mass Spectrom. 19 (2008) 1726.
[14] (a) F. Turecek, J.W. Jones, T. Towle, S. Panja, S.B. Brondsted, P. Hvelplund, B. Paizs, J. Am. Chem. Soc. 130 (2008) 14584;
(b) F. Tureček, C. Yao, Y.M.E. Fung, S. Hayakawa, M. Hashimoto, H. Matsubara, J. Phys. Chem. B 113 (2009) 7347;
(c) F. Tureček, S. Panja, J.A. Wyer, A. Ehlerding, H. Zettergen, S.B. Nielsen, P. Hvelplund, B. Bythell, B. Paizs, J. Am. Chem. Soc. 131 (2009) 16472.
[15] P.B. O'Connor, C. Lin, J.J. Cournoyer, J.L. Pittman, M. Belyayev, B.A. Budnik, J. Am. Soc. Mass Spectrom. 17 (2006) 576.
[16] Y.M.E. Fung, T.-W.D. Chan, J. Am. Soc. Mass Spectrom. 16 (2005) 1523.
[17] D. Moran, R. Jacob, G.P.F. Wood, M.L. Coote, M.J. Davies, R.A.J. O'Hair, C.J. Easton, L. Radom, Helv. Chim. Acta 89 (2006) 2254.
[18] (a) I.K. Chu, J. Zhao, M. Xu, S.O. Siu, A.C. Hopkinson, K.W.M. Siu, J. Am. Chem. Soc. 130 (2008) 7862;
(b) C.-K. Siu, J. Zhao, J. Laskin, I.K. Chu, A.C. Hopkinson, K.W.M. Siu, J. Am. Soc. Mass Spectrom. 20 (2009) 996.
[19] T. Ly, R.R. Julian, J. Am. Soc. Mass Spectrom. 20 (2009) 1148.
[20] T.W. Chung, F. Turecek, J. Am. Soc. Mass. Spectrom 21 (2010), doi:10.1016/j.jasms.2010.02.018.
[21] M.J. Frisch, G.W. Trucks, H.B. Schlegel, G.E. Scuseria, M.A. Robb, J.R. Cheeseman, J.A. Montgomery Jr., T. Vreven, K.N. Kudin, J.C. Burant, J.M. Millam, S.S. Iyengar, J. Tomasi, V. Barone, B. Mennucci, M. Cossi, G. Scalmani, N. Rega, G.A. Petersson, H. Nakatsuji, M. Hada, M. Ehara, K. Toyota, R. Fukuda, J. Hasegawa, M. Ishida, T. Nakajima, Y. Honda, O. Kitao, H. Nakai, M. Klene, X. Li, J.E. Knox, H.P. Hratchian, J.B. Cross, C. Adamo, J. Jaramillo, R. Gomperts, R.E. Stratmann, O. Yazyev, A.J. Austin, R. Cammi, C. Pomelli, J.W. Ochterski, P.Y. Ayala, K. Morokuma, G.A.Voth, P. Salvador, J.J. Dannenberg, V.G. Zakrzewski, S. Dapprich, A.D. Daniels, M.C. Strain, O. Farkas, D.K. Malick, A.D. Rabuck, K. Raghavachari, J.B. Foresman, J.V. Ortiz, Q. Cui, A.G. Baboul, S. Clifford, J. Cioslowski, B.B. Stefanov, G. Liu, A. Liashenko, P. Piskorz, I. Komaromi, R.L. Martin, D.J. Fox, T. Keith, M.A. Al-Laham, C.Y. Peng, A. Nanayakkara, M. Challacombe, P.M.W. Gill, B. Johnson, W. Chen, M.W. Wong, C. Gonzalez, J.A. Pople, Gaussian 03, Revision B.05, Gaussian Inc., Pittsburgh, PA, 2003.
[22] (a) A.D. Becke, J. Chem. Phys. 98 (1993) 1372;
(b) A.D. Becke, J. Chem. Phys. 98 (1993) 5648;
(c) P.J. Stephens, F.J. Devlin, C.F. Chabalowski, M.J. Frisch, J. Phys. Chem. 98 (1994) 11623–11627.
[23] C. Møller, M.S. Plesset, Phys. Rev. 46 (1934) 618.
[24] (a) H.B. Schlegel, J. Chem. Phys. 84 (1986) 4530;
(b) I. Mayer, Adv. Quant. Chem. 12 (1980) 189.
[25] F. Tureček, J. Phys. Chem. A 102 (1998) 4703.
[26] A.E. Reed, R.B. Weinstock, F. Weinhold, J. Chem. Phys. 83 (1985) 735.
[27] R.G. Gilbert, S.C. Smith, Theory of Unimolecular and Recombination Reactions, Blackwell Scientific Publications, Oxford, 1990, pp. 52–132.
[28] L. Zhu, W.L. Hase, Quantum Chemistry Program Exchange;, Indiana University, Bloomington, 1994, Program No. QCPE 644.
[29] A.J. Frank, M. Sadílek, J.G. Ferrier, F. Tureček, J. Am. Chem. Soc. 119 (1997) 12343.
[30] F. Tureček, E.A. Syrstad, J.L. Seymour, X. Chen, C. Yao, J. Mass Spectrom. 38 (2003) 1093.
[31] G. Frison, A. Bull, G. van der Rest, F. Tureček, T. Besson, J. Lemaire, P. Maître, J. Chamot-Rooke, J. Am. Chem. Soc. 130 (2008) 14916.
[32] F. Tureček, T.W. Chung, C.L. Moss, J.A. Wyer, A. Ehlerding, H. Zettergren, S.B. Nielsen, P. Hvelplund, J. Chamot-Rooke, B. Bythell, B. Paizs, J. Am. Chem. Soc. 132 (2010) in press.
[33] (a) B. Paizs, S. Suhai, J. Am. Soc. Mass Spectrom. 15 (2004) 103;
(b) J. Laskin, T.H. Bailey, J.H. Futrell, Int. J. Mass Spectrom. 234 (2004) 89;
(c) J. Laskin, T.H. Bailey, J.H. Futrell, Int. J. Mass Spectrom. 249 (2006) 462;
(d) B.J. Bythell, D.F. Barofsky, F. Pingitore, M.J. Polce, P. Wang, C. Wesdemiotis, B. Paizs, J. Am. Soc. Mass Spectrom. 18 (2007) 1291;
(e) H. Lioe, J.G.E. Reid, R.A.J. O'Hair, J. Phys. Chem. A 111 (2007) 10580;
(f) W.R. Cannon, D. Taasevigen, D.J. Baxter, J. Laskin, J. Am. Soc. Mass Spectrom. 18 (2007) 1625.
[34] M.A. Belyayev, J.J. Cournoyer, C. Lin, P.B. O'Connor, J. Am. Soc. Mass Spectrom. 17 (2006) 1428.
[35] S. Hayakawa, M. Hashimoto, H. Matsubara, F. Tureček, J. Am. Chem. Soc. 129 (2007) 7936.
[36] F. Tureček, X. Chen, C. Hao, J. Am. Chem. Soc. 130 (2008) 8818.